Folding Angles of Degree-4 Rigid Origami

Santure Chen
alkaid_c@outlook.com

May 1, 2024

Abstract

This paper explores the geometrical characteristics of degree-4 vertices in flat-foldable rigid origami. Previous researchers have established relationships between opposite sector angles, opposite folding angles, and adjacent folding angles. However, their proofs tend to be complicated and distant from the geometrical nature of the origami problem. We constructed a proof for the relationship between opposite folding angles that seems to be simpler than proofs that appear in literature; moreover, we proved a theorem, which appears without proof in literature, that may reveal the nature of the mysterious half-angle parameters that appeared in many equations in this field.

Acknowledgement

I had a lot of fantasies for this day. I imagined that my ex-girlfriend would come and ask me to get back together, and I would say no. I imagined that, if I had continued the factorization project with Professor Baeth, two agents from the National Security Agency would come in the middle of the defense and tell me I have to go with them now to crack Russian military cipher, and I would leave the committee a hard decision because I would not finish my defense. Obviously, none of them happened. But when today really comes, I am actually very calm — no excitement, no anxiety, no disappointment, none of any strong emotion. (Edit on May 3rd: Inaccurate; I was actually too nervous to feel any feeling.)

I realize that this is barely my personal showtime. I have been rejected by graduate school in math and decided to go for a master's degree in industrial engineering; there is not much I can do for myself. However, this is a chance to give acknowledgment to those who help me, who believe in me, and who care for me, to tell them that I do become a person that they may feel proud of. I realize that this thesis was only possible because of the abundant love, support, encouragement, model, and inspiration lavished on me by a huge number of people, inside or outside of academia, close or not, responsible for me or not, named or not, whom I would like to acknowledge and offer my sincerest thanks.

I would like to express my deepest gratitude to my supervisor, Professor Thomas Hull, for his tireless, detailed, and insightful guidance day and night, weekdays and weekends. I am also deeply indebted to Professor Annalisa Crannell, Professor Michael McCooey, Professor Barbara Nimershiem, and Professor Ryan Trainor for joining my honor committee and giving me invaluable patience and feedback.

I never thought my talent in math was more than average, but almost everyone around me believed in me and carefully cultivated it. I also frequently doubted the meaning of learning math, but the passion and care that my professors showed me demonstrated how wonderful the mathematician community is. I would have given up the honor, dropped my math major, or even not declared the major without any of Ms. Wenyi Liao, Dr. Quanzhi Ye, Professor Nimershiem, Professor Nicolas R. Baeth, Professor Daniel Droz, Professor Crannell, and Professor Michael McCooey.

As Tech Oh presented at the MAA EPaDel 2024 Spring Conference, math is not only about abstract knowledge but also deeply resonates with the essence of me as a person. I would like to express my deepest appreciation to my grandmother, my parents, Ms. Yixin Wang, Ms. Shuang Lei, Professor Bennett Helm, and many people that have been listed above, who guided me to become a better person. I also want to thank everyone around me for tolerating my mistakes and waiting for me to grow.

I am grateful to my friends who have had a prolonged impact on me and supported me during difficult times, including Xingyuan "Ben" Chen, Jiani Dai, Dr. Nathan Feng, Enzo He, Wei Huang, Cancan Zhang (Ms. V.), Kris Zheng, Hongyi "Big Bro" Liu, Runchen Liu, Shuanwei Tseng, Shaolun Wang, and Ms. Yixin Wang. I also want to recognize the friends who have created a lot of joy

with me and accompanied me day by day, including Liam Connolly, Carol Dong (A'Ag), Tech Oh, Yao Xiao, Xinyuan Zhang, Ruobing Zhao, and online friends I do not know how to address them appropriately.

Besides, several people have served as role models for me, and the admiration has been an important driving factor for my growth, though they may not know their impact on me at all. Because I am not close to some of them, I will list their initials for their privacy: my classmate K. P., my college-house-mate K. D., and Prof. M. M., and some names listed above.

Finally, I must extend my appreciation to the staff at McDonald's, KFC, Popeyes, Royal Farms, Waffle House, Uber Eats, and DoorDash for providing the sustenance that fueled my late-night work sessions, even if it did contribute to an expanding pot belly.

My memory of my undergraduate years may fade, and I may no longer have opportunity to write paper in pure math. However, I know this experience has changed me forever, and will be imperceptibly reflected in every decision I make in the future.

(The names are listed in either alphabetical order or chronological order.)

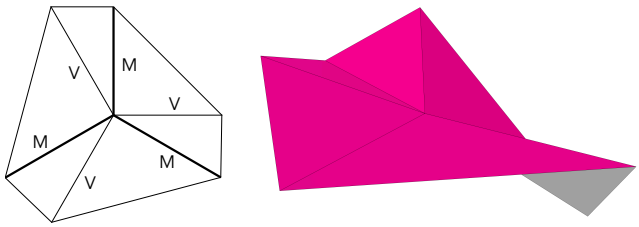

Figure 1: A non-flat-foldable vertex with sector angles 30°, 90°, 30°, 90°, 30°, 90° and creases M, V, M, V, M, V. The right image was created using the Origami Simulator [Gha].

1 Define the Scenario

1.1 General Setting

Origami, as a term in daily life, refers to the Japanese art of folding paper. Mathematically, we say that paper is a planar surface that does not stretch (or compress), and origami is a 3D deformation of paper without intersection with itself.

More specifically, in this paper (no pun intended), we are concerned about rigid origami around one vertex. An origami is considered *rigid* if all facets are flat polygons (which means that all *creases* bordering the facets are straight) and the folding angles can vary continuously. The *folding angle* at a crease describes how much the paper is bent at the crease. A zero folding angle means the paper is unfolded at this crease. Moreover, if the paper extends indefinitely, it will divide the 3D space into two parts. If we observe from a specific side, some creases will look like valleys, while others will look like mountains. And, if we observe from the other side, the mountain will look like a valley and vice versa.

Though folding angles can vary continuously in rigid origami, in some cases, they may only vary within a limited range. We say an origami is *flat-foldable* if all of its folding angles can be $\pm\pi$ simultaneously, i.e., the paper is folded to a flat state. An example of a non-flat-foldable origami vertex is shown in Figure 1.

Lastly, a degree-4 vertex is a point where four creases meet. It is well-known that a flat-foldable rigid origami is only possible if the number of creases at the vertex is an even number no less than 4 [Hul94], so the degree-4 vertex is the simplest possible flat-foldable rigid origami. The relationship among the folding angles of these four creases at the vertex is the subject of our study.

1.2 Notations and formal definitions

More precisely, for a piece of paper $\mathcal{K} \subset \mathbb{R}^2$, an *origami* is a function $f : \mathcal{K} \to \mathbb{R}^3$, that is (a) continuous and (b) a piecewise isometric. ($\mathcal{K}$ is used here, because,

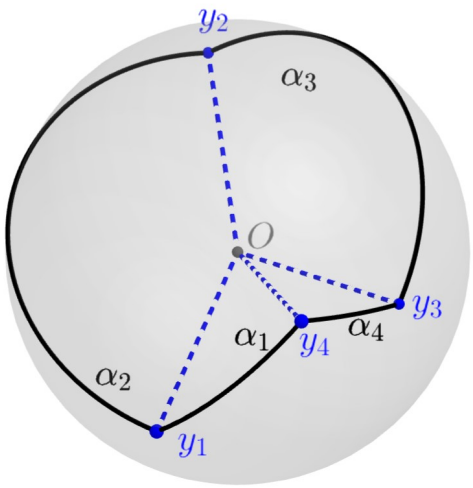

Figure 2: Annotated vertex enclosed by a unit sphere. (All spherical images were made using GeoGebra [Hoh].)

P is occupied by something that will appear later, and *kami* means paper in Japanese.) An *isometry* is a bijection such that, for any line segment $l \subset \mathcal{K}$, $f(l)$ and l have the same length. Then we define the *crease pattern* C of the rigid origami f to be the subset of $\mathcal{K}$ where f is non-differentiable. Other people have proved that under these conditions, C must be a straight-line embedding of a planar graph on $\mathcal{K}$ [Rob78; Hul20].

Figure 2 shows an example of degree-4 flat-foldable rigid origami with labels we will use in this paper. We place the vertex at the center of a unit sphere, and, thereby, creases and sectors can be mapped to their intersections with the sphere. A crease intersects the sphere on a point, and a sector intersects the sphere at an arc.

A basic result of flat origami vertices, known as *Maekawa's Theorem* [KT88] is that the difference between the number of mountain and valley creases at a flat-foldable vertex is always two. For a degree-4 vertex, this means one of the creases is a mountain while three are valleys, or vice-versa. And, as stated before, if we observe from a different side of the paper, mountain(s) will become valley(s) and vice versa. In this paper, we flip the paper until only one crease is the mountain when we observe from the top. We will mark the corresponding point of the mountain crease on the sphere as y_4. In clockwise order, we mark the following creases as y_1, y_2, and y_3.

The four sectors are mapped as four arcs on the sphere. We name the arc between y_4 and y_1 as α_1, and then name the following arcs as α_2, α_3, and α_4 in a clockwise order. The lengths of these arcs are exactly the sector angles of these

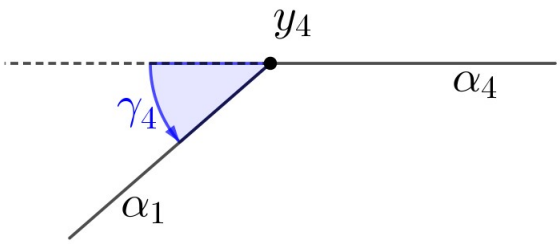

Figure 3: Annotated crease, under a mountain fold.

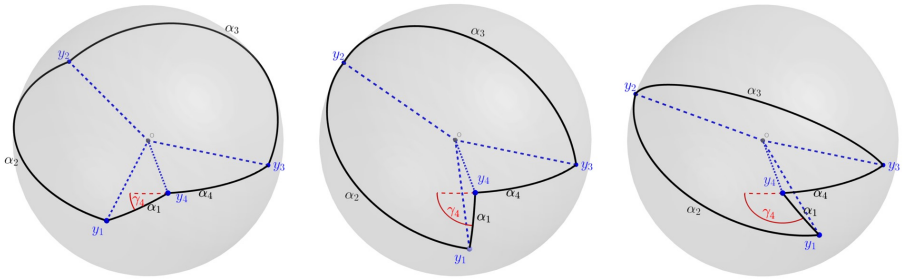

Figure 4: The folding process.

sectors. The range for sector angles is $(0, \pi)$, which will be proved in Section 3.1. Also, the conclusion of Section 3.3 (Equation (25)) indicates that this setting also implies $\alpha_2 \geq \alpha_1$. In this paper, we treat sector angles as given constants, i.e., we study the variation of folding angles with fixed crease patterns.

The folding angles, however, need a more careful definition. We mark the folding angle around crease y_1, y_2, y_3, and y_4 as γ_1, γ_2, γ_3, and γ_4, respectively. Figure 3 shows how the folding angle for crease y_4 is defined, exemplifying how other folding angles are defined. We treat the sector at the counterclockwise side (right side if you view the vertex from the top) as the reference plane. Then the sector at the clockwise (or left) side is seen as bent, or deviated, from the reference plane. In this case, α_1 is bent down (or, counterclockwise, if we view from the crease to the vertex) from the plane where α_4 resides. In this paper, we consider a clockwise bending as a positive folding angle, and a counterclockwise bending as a negative folding angle. This means that the mountain will have a negative folding angle and the valleys will have positive folding angles.

It should be noticed, that the range for folding angles is $[-\pi, \pi]$ to avoid letting the paper intersect with itself. And, for a rigid folding of a degree-4 flat-foldable vertex, because the degree of freedom among the folding angles is 1 [Hul20], we may say that any folding angle is a function of any other folding

angle. For $g : \gamma_a \mapsto \gamma_b$, where γ_a and γ_a are arbitrary folding angles, its domain and range are both $[-\pi, \pi]$. Figure 4 shows how folding angles continuously change.

However, after abstraction, it is very common that folding angles could be represented by a value beyond this range, which is caused by the periodical nature of rotation. If we ignore the limitation imposed by the definition of origami, that the paper cannot intersect with itself, and let the folding angle be x at a given crease, we may also say that this crease is folded $x + 2n\pi$, where $n \in \mathbb{Z}$. Notably, if $0 < x < \pi$, the alternative expression $x - 2\pi$ (with magnitude $2\pi - x$) is especially confusing, because it is exactly the complement of the desired arc on a sphere. Readers may frequently feel they discover a counter-example or an extra solution not mentioned in this paper if they forget that the folding angles and related arcs cannot be longer than π due to the fact that a paper cannot intersect with itself.

For the remainder of this paper, I will use origami to refer to degree-4 rigid flat-foldable origami.

2 The question

In 1976 David Huffman [Huf76] found that one pair of opposite creases will have the same folding angle, while the folding angles for the other pair will have the same value but opposite signs. That is, $\gamma_1 = \gamma_3$, $\gamma_2 = -\gamma_4$. It is a simple and beautiful result. For adjacent angles, we also have a somehow beautiful formula (which has been discovered by several researchers, such as [LMH16]):

$$-\frac{\tan\frac{\gamma_3}{2}}{\tan\frac{\gamma_4}{2}} = \frac{\tan\frac{\gamma_1}{2}}{\tan\frac{\gamma_2}{2}} = \frac{\sin\frac{\alpha_2+\alpha_1}{2}}{\sin\frac{\alpha_2-\alpha_1}{2}}.$$

Noticing that α_1 and α_2 are indeed constant for a given crease pattern, we may say that $\tan\frac{1}{2}\gamma_1$ and $\tan\frac{1}{2}\gamma_2$, as well as $\tan\frac{1}{2}\gamma_3$ and $\tan\frac{1}{2}\gamma_4$, have a simple linear relationship. However, what makes this formula specifically confusing is the geometric meaning of the tangent value of half angles—why does *half* angle matter?

In fact, the original formula that people discovered through geometric means is quite complex (see Equation (24)). However, by substituting with half angles, the equation is dramatically simplified. Taking the tangent of half the folding angles also simplifies several other equations in the field of rigid origami, e.g., [FHR22]. This lets us suspect that the half-angle may indicate an in-depth essence of this field. In this paper, we aim to give a geometrical illustration for this equation, though, unfortunately, this grand goal is still not presently reached.

In what follows, we construct a proof for the relationship between opposite folding angles that seems to be simpler than proofs that appear in literature. In addition we prove a lemma that reveals some geometrical significance of the half-angles, though it is still unclear why it would appear in the relationship between adjacent folding angles.

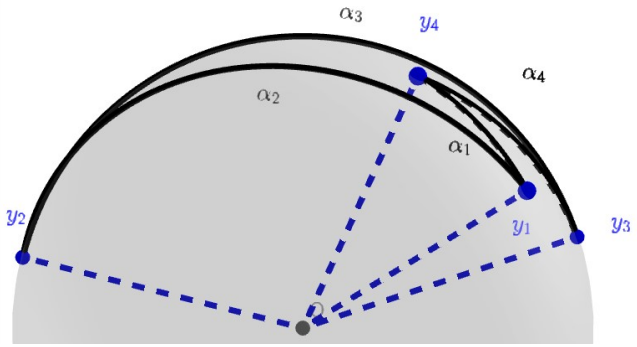

Figure 5: A nearly flat-folded vertex, allowing the relationship among sector angles to be obvious.

3 Existing Literature

We will need to use two basic theorems from flat origami, called the *Kawasaki's* and *Maekawa's* Theorems (see [KT88] and [Hul20]). For completeness, we provide their proofs here.

3.1 Sector Angles: Kawasaki's Theorem

Theorem 3.1. *Opposite sector angles in a flat-foldable degree-4 vertex sum up to π. That is, $\alpha_1 + \alpha_3 = \alpha_2 + \alpha_4 = \pi$.*

Proof. (from [Lan18]) Consider a vertex that is fully flat-folded. That is, the folding angles γ_i are all π or $-\pi$, and all sectors are coplanar, like in Figure 5. Suppose someone is traveling on the edge of the paper, starting at y_1. She travels counterclockwise for α_2, then arrives at y_2; after that, she travels clockwise for α_3, arriving at y_3... and, finally, she comes back to y_1, with a total displacement of 0. It is, thereby, geometrically obvious that

$$\alpha_1 - \alpha_2 + \alpha_3 - \alpha_4 = 0. \tag{1}$$

In other words,

$$\alpha_1 + \alpha_3 = \alpha_2 + \alpha_4. \tag{2}$$

Given that the paper was flat before folding, $\alpha_1 + \alpha_2 + \alpha_3 + \alpha_4 = 2\pi$. Solving this equation system, we have

$$\alpha_1 + \alpha_3 = \alpha_2 + \alpha_4 = \pi. \tag{3}$$

□

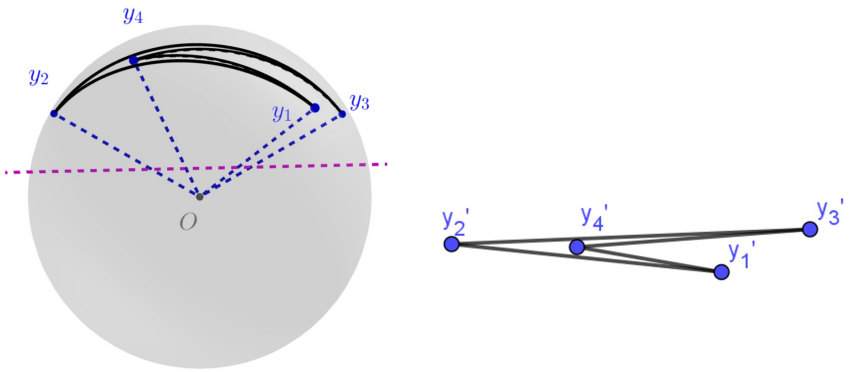

Figure 6: A nearly flat-folded vertex that is cut off by a plane.

3.2 Maekawa's Theorem

Theorem 3.2. *The difference between the number of mountains and the number of valleys in a flat-foldable vertex must be 2.*

Proof. (from [Hul94]) Suppose the vertex has n total creases with m mountains and v valleys. therefore, $n = m + v$. Let a plane intersect with all the creases without intersecting the vertex. The intersection forms a polygon with n sides, and each as shown in Figure 6. The sum of internal angles of n polygon is $(n - 2)\pi$. When the vertex is fully flat-folded, the internal angles around mountain creases will be 2π, and the internal angles around valley creases will be 0. So the sum of internal angles is also $2m\pi + 0v$. Solving these equations, we will have $v - 2 = m$. □

3.3 Opposite Folding Angles

Theorem 3.3. *The opposite folding angles in a rigid folding of a degree-4 flat-foldable vertex have the same magnitude.*

Specifically, because we have 3 positive angles and 1 negative angle by Maekawa's Theorem, one opposite pair of the folding angles will be equal while the other pair will have equal magnitudes but opposite signs. A spherical trigonometry proof can be found in the literature [Lan18], which follows.

Proof. As shown in Figure 7, connect y_4 and y_2 by line segment ζ. Then, in the triangle $\triangle y_2y_3y_4$, considering the spherical cosine law [BEG99, p. 348], we have

$$\cos(\zeta) = \cos(\alpha_3)\cos(\alpha_4) + \sin(\alpha_3)\sin(\alpha_4)\cos(\pi - \gamma_3). \tag{4}$$

And, for the same reason, in the triangle among y_2, y_4, and y_1, we have

$$\cos(\zeta) = \cos(\alpha_1)\cos(\alpha_2) + \sin(\alpha_1)\sin(\alpha_2)\cos(\pi - \gamma_1). \tag{5}$$

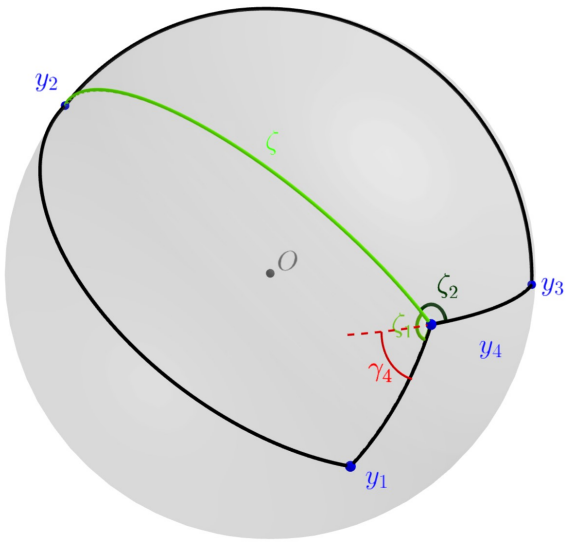

Figure 7: a vertex with ζ that connects y_2 and y_4. Several angles around y_4 are emphasized for clarity of proof in section 3.4. If These labels cannot satisfy you and you need more information, please refer to Figure19 in the appendix.

Notice, by Equation (3), $\alpha_1 = \pi - \alpha_3$, and $\alpha_2 = \pi - \alpha_4$. Substituting them gives,

$$\cos(\alpha_3)\cos(\alpha_4) + \sin(\alpha_3)\sin(\alpha_4)\cos(\pi - \gamma_3)$$
$$= \cos(\pi - \alpha_3)\cos(\pi - \alpha_4) + \sin(\pi - \alpha_3)\sin(\pi - \alpha_4)\cos(\pi - \gamma_1)$$

Simplifying the equation using the periodical nature of sine and cosine functions, we have

$$\cos(\pi - \gamma_3) = \cos(\pi - \gamma_1). \tag{6}$$

Considering the range of folding angles is $[-\pi, \pi]$,

$$\gamma_3 = \pm\gamma_1. \tag{7}$$

The same argument also applies to γ_2 and γ_4. Because there must be three positive and one negative folding angles, one pair will have the opposite signs and the other pair will have the same sign. In our particular notation, γ_4 is negative while γ_1, γ_2, and γ_3 are positive, so $\gamma_1 = \gamma_3$ and $\gamma_2 = -\gamma_4$. □

Though this proof is short and straightforward, a more visual and geometrical proof is possible using the Gauss map, as we will see in Section 4.1.

3.4 Adjacent Folding Angles

Theorem 3.4. *The following equation that relates adjacent folding angles and adjacent sector angles in a rigid folding of a flat-foldable, degree-4 vertex holds:*

$$\frac{\tan\frac{\gamma_1}{2}}{\tan\frac{\gamma_2}{2}} = \frac{\sin\frac{\alpha_2+\alpha_1}{2}}{\sin\frac{\alpha_2-\alpha_1}{2}}.$$

Proof. (from [Lan18]) As shown in Figure 7, let $\zeta_1 = \angle y_2y_4y_1$, and $\zeta_2 = \angle y_2y_4y_3$. Considering the definition of folding angle that was stated in Section 1.2, the magnitude of folding angle γ_4 can be represented as $\zeta_1 + \zeta_2 - \pi$. This gives us

$$-\sin\gamma_4 = \sin\zeta_1\cos\zeta_2 + \sin\zeta_2\cos\zeta_1 \tag{8}$$

By the spherical sine and cosine law [BEG99, p. 348], we have

$$\frac{\sin\zeta_1}{\sin\alpha_2} = \frac{\sin\gamma_1}{\sin\zeta} \tag{9}$$

$$\frac{\sin\zeta_2}{\sin\alpha_3} = \frac{\sin\gamma_3}{\sin\zeta} \tag{10}$$

$$\cos\zeta_1\sin\alpha_1\sin\zeta = \cos\alpha_2 - \cos\alpha_1\cos\zeta \tag{11}$$

$$\cos\zeta_2\sin\alpha_4\sin\zeta = \cos\alpha_3 - \cos\alpha_4\cos\zeta. \tag{12}$$

Isolating $\sin\zeta_1$, $\sin\zeta_2$, $\cos\zeta_1$, and $\cos\zeta_2$ from the equations above, we have

$$\sin\zeta_1 = \frac{\sin\alpha_2\sin\gamma_1}{\sin\zeta}, \tag{13}$$

$$\sin\zeta_2 = \frac{\sin\alpha_3\sin\gamma_3}{\sin\zeta}, \tag{14}$$

$$\cos\zeta_1 = \frac{\cos\alpha_2 - \cos\alpha_1\cos\zeta}{\sin\alpha_1\sin\zeta}, \text{ and} \tag{15}$$

$$\cos\zeta_2 = \frac{\cos\alpha_3 - \cos\alpha_4\cos\zeta}{\sin\alpha_4\sin\zeta}. \tag{16}$$

Utilizing results of Theorem 3.1 and 3.3, we can eliminate variables α_3, α_4, γ_3, and γ_4:

$$\sin\zeta_1 = \frac{\sin\alpha_2\sin\gamma_1}{\sin\zeta}, \tag{17}$$

$$\sin\zeta_2 = \frac{\sin\alpha_1\sin\gamma_1}{\sin\zeta}, \tag{18}$$

$$\cos\zeta_1 = \frac{\cos\alpha_2 - \cos\alpha_1\cos\zeta}{\sin\alpha_1\sin\zeta}, \text{ and} \tag{19}$$

$$\cos\zeta_2 = -\frac{\cos\alpha_1 - \cos\alpha_2\cos\zeta}{\sin\alpha_2\sin\zeta}. \tag{20}$$

Substituting them into Equation (8), we have

$$\sin\gamma_2 = \frac{\sin\alpha_2\sin\gamma_1}{\sin\zeta}\frac{\cos\alpha_1-\cos\alpha_2\cos\zeta}{\sin\alpha_2\sin\zeta} - \frac{\sin\alpha_1\sin\gamma_1}{\sin\zeta}\frac{\cos\alpha_2-\cos\alpha_1\cos\zeta}{\sin\alpha_1\sin\zeta}. \tag{21}$$

Simplifying this equation, we will get

$$\sin\gamma_2 = -\sin\gamma_1\frac{(\cos\zeta+1)(\cos\alpha_2-\cos\alpha_1)}{\sin^2\zeta}. \tag{22}$$

Multiplying both the numerator and denominator by $\cos\zeta-1$, then considering the Pythagorean identity, we can simplify it as

$$\sin\gamma_2 = -\sin\gamma_1\frac{\cos\alpha_2-\cos\alpha_1}{1-\cos\zeta}. \tag{23}$$

Then by substituting $\cos\zeta$ from Equation (5), we eventually end up with this Frankenstein equation:

$$\sin\gamma_2 = -\sin\gamma_1\frac{\cos\alpha_2-\cos\alpha_1}{1-(\cos\alpha_1\cos\alpha_2-\sin\alpha_1\sin\alpha_2\cos\gamma_1)}. \tag{24}$$

However, magically, once we employ the Weierstrass substitution, the following linear relationship that is too simple to be not arbitrary appears in front of us:

$$\frac{\tan\frac{\gamma_1}{2}}{\tan\frac{\gamma_2}{2}} = \frac{\sin\frac{\alpha_2+\alpha_1}{2}}{\sin\frac{\alpha_2-\alpha_1}{2}}. \tag{25}$$

And, given the conclusion of Section 3.3, γ_3 and γ_4 also have a similar relationship. □

3.5 Gauss Map

For a curve C on a 2D surface in 3D space, a Gauss map $G : C \to S_2$ is a function that maps every point on C to a unit vector orthogonal to the surface at that point. Letting the vector's initial point be the origin will enable us to represent this vector by a point on the unit sphere S_2. If the curve C is differentiable, then the mapped curve $C' = G(C)$ will form a continuous curve on the unit sphere, and, if C is closed, the mapped curve C' will also be closed.

It might become tricky when the curve is not differentiable - for example, when the curve passes through a sharp corner, such as a crease line. In this case, we define the map of this point as the shortest path between the mapped points of the point "right before" and "right after" this point. (Limits will be used in the formal definition, of course.) On the one hand, it maintains the continuity of the image curve C' by the shortest path; on the other hand, all points on this path are orthogonal to the sharp corner, which does not violate the definition of the Gauss Map.

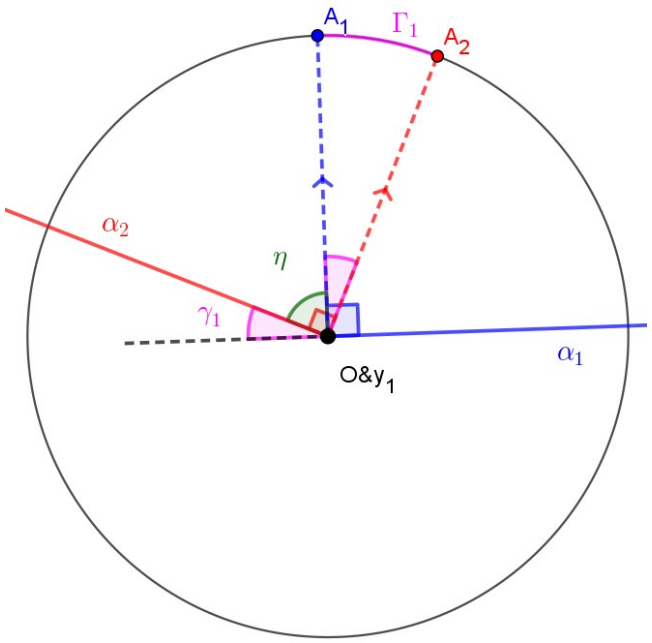

Figure 8: View from the side, so that crease y_1 and vertex O overlapping.

3.5.1 Gauss Map for Degree-4 Vertex

In this paper, we pay attention to the Gauss Map of a closed curve around our rigidly folded vertex. Obviously, a sector will be mapped as a point, because the sector is flat, and the creases will map to line segments that connect them. Given there are 4 sectors and 4 creases, the Gauss map image will form a quadrilateral shape.We accordingly name the map of four sectors as A_1, A_2, A_3, and A_4, respectively, and the map of four creases as Γ_1, Γ_2, Γ_3, and Γ_4, respectively.

Figure 8 shows how the mapping looks from the side. In this particular graph, we view it from a point on the crease y_1 and look towards the vertex. The sectors α_1 and α_2 are mapped to points A_1 and A_2, respectively, and the arc Γ_1 connects point A_1 and A_2 because crease y_1 borders sectors α_1 and α_2. From this graph, you may easily see the two pink angles, $\angle\gamma_1$ and $\angle A_1OA_2$ have the same value: A_1O and α_1 are perpendicular, so $\angle\eta + \gamma_1 = \frac{\pi}{2}$; A_2O and α_2 are perpendicular, so $\angle\eta + \angle A_1OA_2 = \frac{\pi}{2}$. Because Γ_1 is an arc on a unit sphere, its length is exactly the size of $\angle A_1OA_2$ expressed in radians. So we say that $\Gamma_1 = \angle A_1OA_2 = \gamma_1$. A similar argument applies to every folding angle, so $\Gamma_i = \angle\gamma_i$ for all $i = 1, 2, 3, 4$.

For Sector angles, the situation is a little bit complex. As Figure 9 shows, due to different relative positions, when we apply the similar technique we used in the paragraph above, $\angle A_1A_2A_3 = \pi - \alpha_2$, but $\angle A_3A_4A_1 = \alpha_4$. Noticing Theorem 3.1 indicates that $\pi - \alpha_2 = \alpha_4$, we have $\angle A_1A_2A_3 = \angle A_3A_4A_1$. The

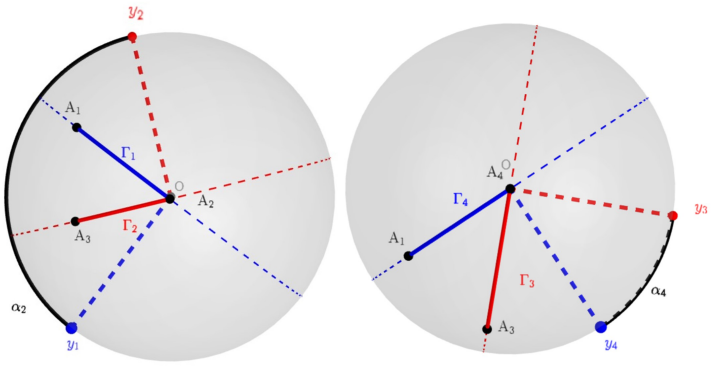

Figure 9: View from the top, so in the left picture A_2 and vertex O are overlapping, and in the right picture A_4 and$O$ are overlapping.

same process allows us get $\angle A_2A_3A_4 = \angle A_4A_1A_2$.

And, as shown in Figure 10, the Gauss map image C' will be a bow tie-ish shape, i.e., a pair of opposite sides will cross each other, when it is neither fully folded nor flat. We will talk about its cause and implication in the following section.

When the paper is not folded at all, then all the surfaces face straight up, causing the Gauss Map to concentrate on one point, as shown in the right part of Figure 11.

When the paper is fully folded, then sector α_2 and α_4 face straight up, while α_1 and α_3 face straight down. They will concentrate at the north and south poles. Then, Γ_is become half-circles orthogonal to the corresponding ray y_i, respectively. Consequentially, the Gauss Map becomes a combination of two *spherical lunes*, as shown in the left part of Figure 11.

3.6 Gauss Curvature

It is trivial that, for a closed curve on a flat surface, the area enclosed by its Gauss map image curve C' is zero. We define the ratio between the area enclosed by the original curve and the image curve to be the *curvature* of the surface at that point. Indeed, this ratio reflects a property of the surface. The *Gauss Curvature* K of a surface at a point P is defined as

$$K(P) = \lim_{C \to P} \frac{E(C')}{E(C)}$$

where C is a closed curve that encloses P and C' is the Gauss Map of C. $E(C)$ and $E(C')$ represents the area, or spherical excess, enclosed by C and C' on their respective surfaces. $\lim_{C \to P}$ means that every point on C is close enough to P. A circle (or, for non-flat surface, the intersection of a sphere and the surface) with center P and radius $r \to 0$ is a curve that satisfies this requirement.

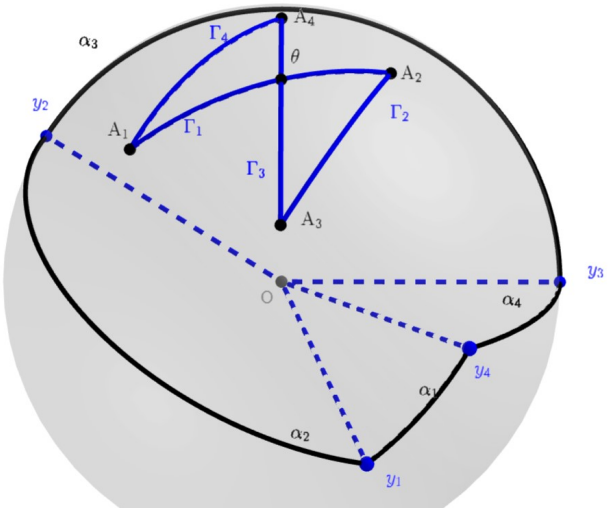

Figure 10: the Gauss Map around vertex, with notations that will be extensively used below.

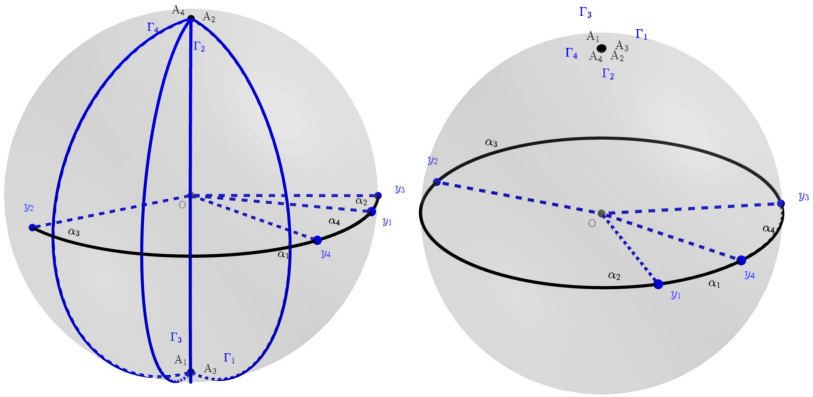

Figure 11: Two degenerate cases for the Gauss Map.

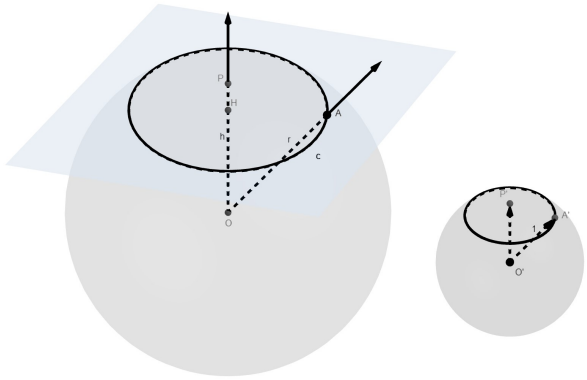

Figure 12: a sphere and its Gauss map

Moreover, if the area is enclosed by a clockwise curve, we say it is positive; while if the area is enclosed by a counterclockwise curve, we say its area is negative. For example, the area of the two triangles that made up the bow tie in Figure 10, must have opposite signs.

A sphere with radius r, for example, has a positive curvature $\frac{1}{r^2}$, and a saddle has a negative curvature.

3.6.1 Gauss Curvature of a Sphere

In this section, I will prove the Gauss curvature of a sphere with radius r is $\frac{1}{r^2}$.

Consider an arbitrary point P on a sphere with center O and radius r, as shown in Figure 12. Let a plane be perpendicular to line PO and intersect with the plane at a circle c. This plane also intersects with line PO at point H. Let h denote the distance between O and H.

Consider an arbitrary point A on the circle c. By trigonometry in triangle $\triangle HOA$, angle $\angle POA = \angle HOA = \arccos(h/r)$. Then the spherical cap enclosed by circle c on sphere O has area $E = 2\pi r^2(1 - \cos(\angle POA)) = 2\pi r^2(1 - h/r)$.

Let there be a unit sphere with center O' and radius 1. Using the Gauss map to map P, c, and A to this sphere, we have their image P', c' and A'. Because vector OA is exactly perpendicular to the sphere O at point A and vector OP is exactly perpendicular to the sphere O at point P, $O'A'$ is parallel to OA, and $O'P'$ is parallel to OP, which means that $\angle POA = \angle P'O'A'$. Then by the same argument, the spherical cap enclosed by circle c' on sphere O' has area $E' = 2\pi(1 - \cos(\angle POA)) = 2\pi(1 - h/r)$.

When h approximates r, circle c will approximate P. Therefore, the Gauss curvature of sphere O at point P is

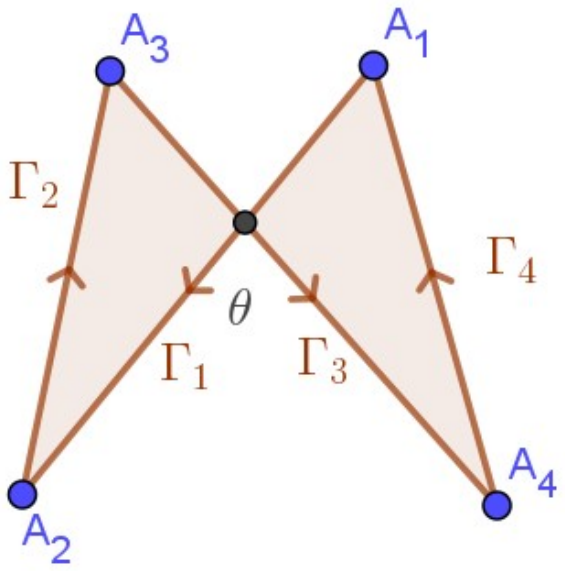

Figure 13: the Gauss Map, with the direction of the curve clearly marked.

$$K(P) = \lim_{h \to r} \frac{E'}{E} = \frac{2\pi(1 - h/r)}{2r^2\pi(1 - h/r)} = \frac{1}{r^2}.$$

3.6.2 Gauss' Remarkable Theorem and Origami

Remarkably, Gauss's Remarkable Theorem (Gauss' Theorema Egregium) states that the Gauss curvature of a surface is *invariant* under a local isometry [ONe66, Theorem 5.4, p. 273]. Isometries, defined as distance-preserving deformations, include origami. Therefore, the Gauss curvature of every vertex discussed in this paper is always 0, i.e., the area enclosed by the mapped curve of any curve that is on the paper and encloses the vertex should be 0.

The bow tie, as shown in Figure 10, seemingly have a non-zero area. However, we must consider that the signs of the two triangles are opposite. As shown in Figure 13, one triangle in the bow tie is enclosed by a clockwise curve, while another is enclosed by a counterclockwise curve. This indicates that the sign of their area is the opposite. This allows the bow tie to have a zero area, and Gauss's Remarkable Theorem does guarantee a zero area, implying so the magnitude of the areas of the two triangles is the same.

In the degenerate case where the paper is fully folded, we can use Theorem 3.1 to easily prove that the two spherical lunes have the same area in magnitude.

4 Original works

4.1 A geometrical proof for opposite folding angles using Gauss Map

As shown in Figure 13, we name the intersection of Γ_1 and Γ_3 as θ. In Section 3.5.1 we proved that $\angle A_2A_3A_4 = \angle A_4A_1A_2$ and $\angle A_1A_2A_3 = \angle A_3A_4A_1$. We also have $\angle A_4\theta A_1 = \angle A_2\theta A_3$, because they are opposite angles. These are sufficient conditions for spherical triangle $\triangle A_4A_1\theta$ and $\triangle A_2A_3\theta$ to be congruent. (since AAA triangle relations give congruent triangles on the sphere). Then $|\Gamma_4| = |\Gamma_2|$, and $|\Gamma_1| = |\Gamma_3|$ because $|A_4\theta| = |A_2\theta|$ and $|A_1\theta| = |A_3\theta|$. So, Theorem 3.3 is proved.

Actually, the bow tie is fully symmetric through the great cricle that contains the midpoint of A_1A_3 and A_2A_4.

4.2 Colinearity of half angles on Gauss Map

The following theorem was first stated by David Huffman [Huf76], but without a proof. Later references to this result, such as [Lan18] also do not include a proof. Because of its potential importance for understanding half angles in rigid origami vertices, we provide a proof here.

Theorem 4.1. *In the Gauss map image of a rigid folding of a degree-4 vertex, the midpoints of bow tie sides Γ_1, Γ_2, Γ_3, and Γ_4 are colinear.*

As we defined before, Γ_1, Γ_2, Γ_3, and Γ_4 are the corresponding arcs of folding angles γ_1, γ_2, γ_3, and γ_4, respectively, on the Gauss sphere. Therefore, the midpoints of these arcs are equivalent to bisectors of folding angles. Their colinearity may facilitate a direct proof of the half-angle formula.

To prove this theorem, we need 2 lemmas.

Lemma 1. *For a spherical triangle $\triangle ABC$ with all sides shorter than π and a line e intersecting it but not tangent to it, $|e, A| = |e, B| = |e, C|$, if and only if e passes through two midpoints of the side of $\triangle ABC$.*

Here $|e, A|$ denotes the shortest distance from a point on the great circle e to the point A.

Proof. First, we will prove that if e passes through two midpoints of the side of $\triangle ABC$ then $|e, A| = |e, B| = |e, C|$.

Let the midpoint of AB and AC be P and Q, respectively, then let e be the great circle (line) passing through PQ. Let three lines be perpendicular with e and pass through B, A, and C, respectively. Name the intersection of these lines and e as M, L, and N, respectively. This set up, as shown in Figure 14, means that$|B, e| = |MB|$, $|C, e| = |CN|$, and $|A, e| = |AL|$

In $\triangle QNC$, by the spherical Law of Sines we have $\frac{\sin\angle Q}{\sin|NC|} = \frac{\sin\angle N}{\sin|QC|}$, or $\sin|NC| = \frac{\sin\angle Q\sin|QC|}{\sin\angle N}$. Given $\angle N = \frac{\pi}{2}$,

$$\sin|NC| = \sin\angle Q\sin|QC|. \tag{26}$$

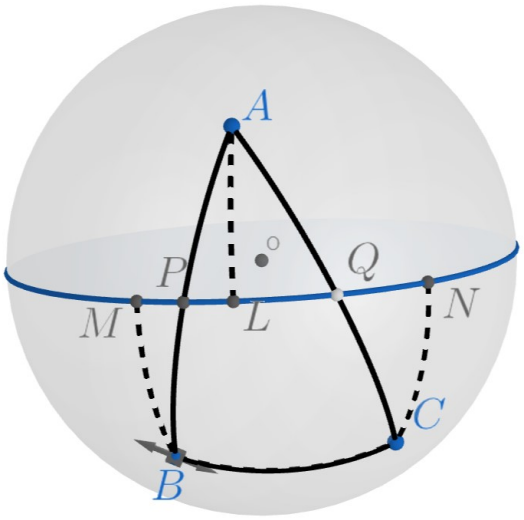

Figure 14: Set up for the first half of the proof of Lemma 1, assuming P and Q are midpoints.

By the same argument, in $\triangle MPB$ and $\triangle APL$, we have

$$\sin|MB| = \sin\angle P \sin|PB|, \tag{27}$$

and

$$\sin|AL| = \sin\angle P \sin|AP|, \tag{28}$$

respectively.

Now, in $\triangle APQ$ by the sine rule we have $\frac{\sin\angle P}{\sin|AQ|} = \frac{\sin\angle Q}{\sin|AP|}$. Alongside with $|AQ| = |QC|$ and $|AP| = |PB|$, this gives us $\sin\angle P \sin|PB| = \sin\angle Q \sin|QC|$. Plugging in Equations (26) and (27), we have

$$\sin|MB| = \sin|NC|. \tag{29}$$

We may notice that $\angle APQ = \angle BPM$ because they are a pair of vertical angles. Besides, considering $|BP| = |AP|$, and Equations (27) and (28), we have

$$\sin|AL| = \sin|MB|. \tag{30}$$

Equations (29) and (30) give us $\sin|MB| = \sin|NC| = \sin|AL|$. Noticing $|PB| \geq |e, B| = |MB|$, and $|PB| = \frac{|AB|}{2} \leq \frac{\pi}{2}$, we have $0 \leq |MB| \leq \frac{\pi}{2}$. Similarly, $0 \leq |NC| \leq \frac{\pi}{2}$ and $0 \leq |AL| \leq \frac{\pi}{2}$. Because sine is a strictly monotone function within the range 0 to $\frac{\pi}{2}$, we have $|MB| = |NC| = |AL|$. This completes our proof of the first half of the lemma.

Now, we will prove that if $|e, A| = |e, B| = |e, C|$ then e passes through two midpoints of the side of $\triangle ABC$, as shown in Figure 15

Without loss of generality, we assume e passes through AB and AC at P and Q, respectively. Let three lines be perpendicular with e and pass through B, A, and C, respectively. Name the intersection of these lines and e as M, L, and N, respectively. This set up, as shown in Figure 15, means that $|B, e| = |MB|$, $|C, e| = |CN|$, and $|A, e| = |AL|$.

In $\triangle QNC$, by the sine rule, we again have $\frac{\sin\angle NQC}{\sin|NC|} = \frac{\sin\angle N}{\sin|QC|}$. Given $\angle N = \frac{\pi}{2}$,

$$\sin|QC| = \frac{\sin|NC|}{\sin\angle NQC}. \tag{31}$$

Similarly, in $\triangle AQL$, we have

$$\sin|AQ| = \frac{\sin|AL|}{\sin\angle AQL}. \tag{32}$$

Because $|AL| = |NC|$ and $\angle AQL = \angle CQN$, we have $\sin|AQ| = \sin|QC|$.

In the case that $|AQ| \leq \frac{\pi}{2}$ and $|QC| \leq \frac{\pi}{2}$, because sin is a strictly monotone function within the range 0 to $\frac{\pi}{2}$, we have $|AQ| = |QC|$, implying Q is the midpoint of AC.

In the case that one of $|AQ|$ is less than or equal to $\frac{\pi}{2}$, and the other is greater than or equal to $\frac{\pi}{2}$ but less than or equal to $\frac{3}{2}\pi$, we have $|AQ|+|QC| = \pi$, which means that $|AC| = \pi$, contradict with the premise of this lemma.

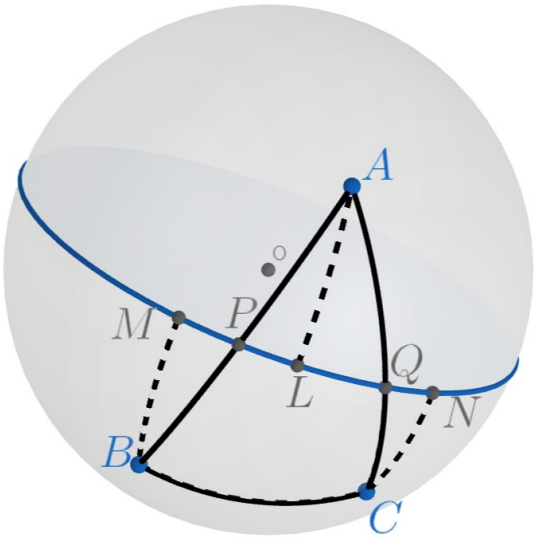

Figure 15: Set up for the second half of the proof of Lemma 1, which does not assume P and Q are midpoints.

By the same argument, we can prove that, in the case $\triangle ABC$ exists, P is the midpoint of AB. This completes our proof of the second direction, and thus completes the whole proof. □

The next lemma is an old spherical geometry result stated in [Tod14], with proof, but with a flaw. Therefore we include a revised statement and proof here. This is not the strongest statement we could prove, but is sufficient for supporting the grand goal of this paper.

Lemma 2. *Let $\triangle ABC$ be a spherical triangle on a unit sphere. Then there exists a small (i.e., not great) circle, called Lexell's circle, such that for any point D on Lexell's circle and on the same side of the great circle made by arc BC as A, we have that the spherical area of $\triangle DBC$ equals the area of $\triangle ABC$. The Lexell's circle is defined by point A, the antipodal point of B, and the antipodal point of C.*

Proof. Let there be a spherical triangle ABC. Then let the antipodals of B and C be B' and C', respectively. Any great circle that passes through B must also pass through B', so do C and C'. We also mark the antipodal point of A as K. Besides, Let P be the center of circumcircle of $\triangle AB'C'$, i.e., $|PA| = |PB'| = |PC'|$, as shown in Figure 16.

We are going to prove that every triangle with it apex on the Lexell's circle has the same area, $2\angle PB'C' - \pi$. Let's use $\triangle ABC$ as an example.

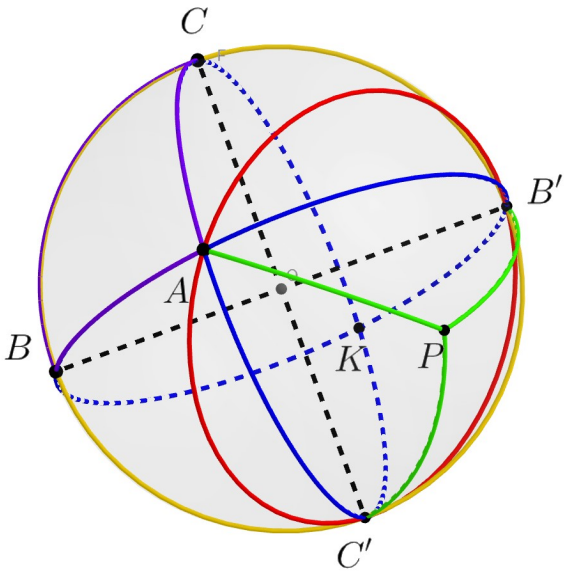

Figure 16: set up of Lemma 2.

Let the area of $\triangle ABC$ be

$$E = \angle BAC + \angle ABC + \angle ACB - \pi. \tag{33}$$

We aim to prove that $E = 2\angle PB'C' - \pi$. $\angle AC'B' = \angle BC'K$ because they are opposite angles. $\angle BC'K = \angle BCK$ because they are both the dihedral angle between the plane defined by B,C, C' and the plane defined by K, C, C'. Now, because $\angle BCK$ and $\angle ACB$ supplementary angles, $\angle BCK = \pi - \angle ACB$. Combining all these steps, $\angle AC'B' = \pi - \angle ACB$. By the same argument, $\angle AB'C' = \pi - \angle ABC$. We also have $\angle BAC = \angle B'AC'$ because they are opposite angles.

Substituting these into Equation (33), we have

$$\begin{aligned} E &= \angle BAC + \angle ABC + \angle ACB - \pi \\ &= \angle B'AC' + (\pi - \angle AB'C') + (\pi - \angle AC'B') - \pi \qquad (34) \\ &= \angle B'AC' - \angle AB'C' - \angle AC'B' + \pi. \qquad (35) \end{aligned}$$

In isosceles triangle $\triangle B'C'P$,

$$\angle B'C'P = \frac{\angle B'C'P + \angle B'C'P}{2} = \frac{\angle C'B'P + \angle B'C'P}{2}. \tag{36}$$

Next we chase some angle in Figure 16 to get

$$\frac{\angle C'B'P + \angle B'C'P}{2} = \frac{\angle AB'C' - \angle AB'P + \angle AC'B' - \angle AC'P}{2}$$
$$= \frac{\angle AB'C' + \angle AC'B' - \angle BAC}{2}. \tag{37}$$

Combining Equation (36) and 37, we have

$$\angle B'C'P = \frac{\angle AB'C' + \angle AC'B' - \angle BAC}{2}. \tag{38}$$

Noticing that the numerator of the right-hand side is similar to the right hand side of the Equation (35), we may have

$$\frac{\angle AB'C' + \angle AC'B' - \angle BAC}{2} = \frac{\pi - E}{2}. \tag{39}$$

Substitute in Equation , we have

$$\angle B'C'P = \frac{\pi - E}{2}. \tag{40}$$

Isolating E from the equation (or, in other word, solving the equation for E, we arrive

$$E = 2\angle PB'C' - \pi. \tag{41}$$

For any point D on the sphere, it satisfies $|PD| = |PC'| = |PB'|$, then by the same argument, the area of triangle $\triangle DBC = 2\angle PB'C' - \pi = \triangle ABC$. This means that every point on Lexell's circle can serve as an apex for a triangle that has the same area as $\triangle ABC$ and share the same base BC.

□

Theorem 4.2. *For spherical triangles, $\triangle ABC$ and $\triangle DBC$ with all sides shorter than π that share the same base and non-zero overlapping area, the midpoints of their distinct sides are colinear if they have the same area.*

Proof. Assume we are given triangles $\triangle ABC$ and $\triangle DBC$ as stated in the Theorem. Let B' and C' be antipodal to B and C, respectively. Then by Lemma 2, A, D, B', and C' are on a small circle l.

Let the line that crosses the midpoint of AB and AC be e. By Lemma 1, $|e, A| = |e, B| = |e, C|$. Because B', and C' are antipodal to B and C, respectively, $|e, B| = |e, B'|$, and $|e, C| = |e, C'|$. Therefore, $|e, A| = |e, B'| = |e, C'|$. This means that the plane that e resides on is parallel to the plane that l resides on, which further means that $|L, e|$ is a constant for all $L \in l$, including D. This gives us $|e, D| = |e, A|$, and then $|e, D| = |e, B| = |e, C|$.

Given the plane that e resides on is parallel to the plane that l resides on, if we divide the sphere by e, all $L \in l$, including A and D will be in one hemisphere. Noticing line segment AB crosses e, we can say that A and B are on two different hemispheres. This means D and B are on two different side of

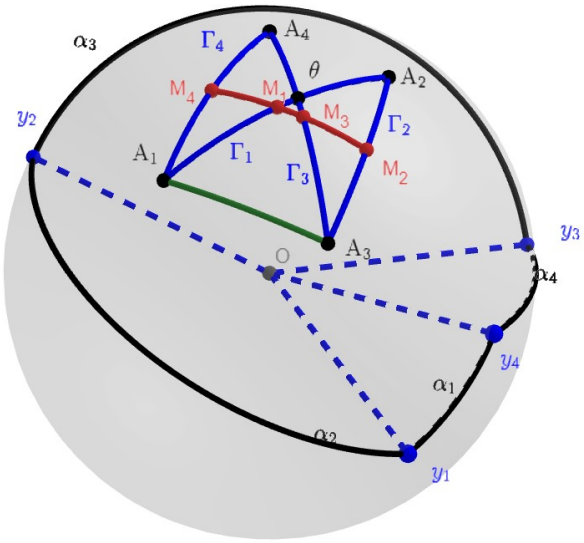

Figure 17: the Gauss Map, with elements mentioned in Theorem 4.1 clearly marked.

e, leading to the conclusion that e intersects with line segment DB. Then by Lemma 1, the midpoint of DB and DC is on e. So the midpoint of AB, AC, DB, and DC are all on e, which completes our proof. □

Now, we are finally eligible to prove Theorem 4.1.

Theorem 4.1 (restate) *In the Gauss map image of a rigid folding of a degree-4 vertex, the midpoints of bow tie sides* Γ_1, Γ_2, Γ_3, *and* Γ_4 *are colinear.*

Proof. When the paper is neither flat nor fully folded, as in Figure 10, connect A_1 and A_3 in the Gauss map, as Figure 17 shows. For convenience, we name the intersecting point of Γ_1 and Γ_3 as θ. As mentioned in Section 3.6.2, the two parts of the bow tie, $\triangle\theta A_2 A_3$ and $\triangle\theta A_1 A_4$, have the same area. Adding with the shared part $\theta A_1 A_3$, then $\triangle A_1 A_3 A_4$ and $\triangle A_1 A_3 A_2$ have the same area, same base, and non-zero overlapping area, fulfilling conditions required in Theorem 4.2. This means that the midpoints of Γ_1, Γ_2, Γ_3, and Γ_4 are colinear.

When the paper is fully folded, as discussed in Section 3.5, the Gauss Map becomes a combination of spherical lunes, as shown in Figure 11. Then the midpoint of Γ_1, Γ_2, Γ_3, and Γ_4 are all on the equator, and, therefore, colinear, as shown in Figure 18.

When the paper is flat, the Gauss Map becomes a point, as shown in Figure 11, where all A_1, A_2, A_3, A_4, Γ_1, Γ_2, Γ_3, and Γ_4 are all overlapping together, so do those midpoints. So the midpoints are also colinear, as shown in Figure 18. □

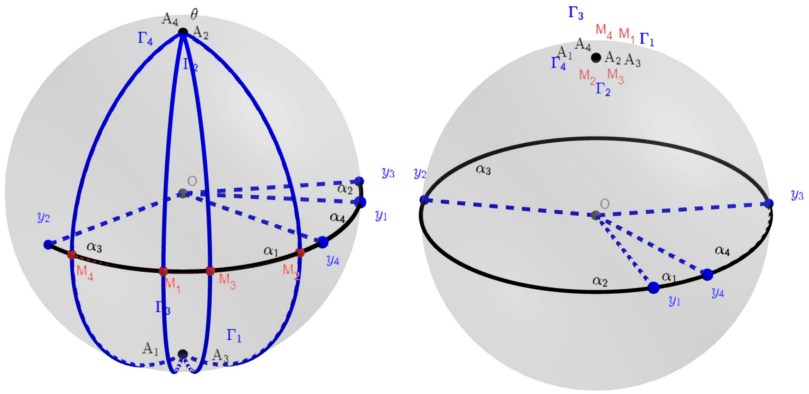

Figure 18: Two degenerate cases for Theorem 4.2.

5 Conclusion

In this paper, I outlined existing studies for the relationship among folding angles and sector angles, then gave a simpler proof for an established relationship, and proved a theorem, which was mentioned in the literature but seemingly never proved, relating half-angles of four folding angles. We also have several other failed attempts that leave nothing worth documenting. Until now, we are still unsure how this may help us understand the relationship between adjacent folding angles. One possible path for breakthrough is to relate the half-angles of the sector angles, which appear on the other side of the equation.

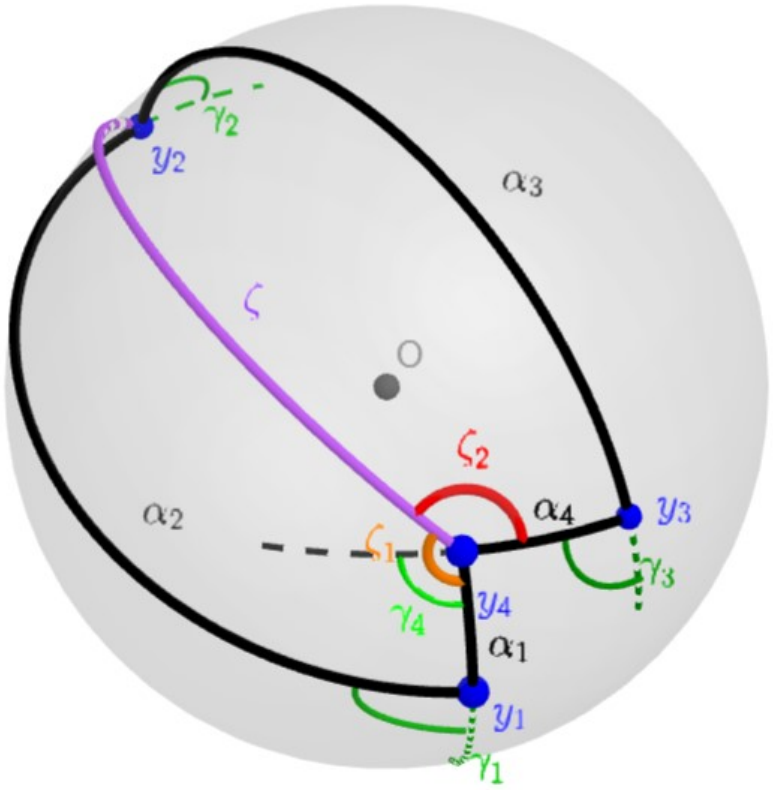

Figure 19: Figure7 with more details.

6 Quick Reference

Listed below are some pieces of information you may want to have in hand when you read through the paper.

6.1 Extra Graph

Figure 19 is Figure7 with more details as requested. It is not provided in the original place because too much information make it look chaotic.

6.2 Definitions

Here we list some definitions and terminologies scattered around the paper.

6.2.1 Origami

- **Origami** is a 3D isometric deformation of a plane without intersection with itself.
- **Flat-foldable** means means the origami can have all of its creases be folded all the way flat.
- **Rigid**, when the folded surface is either flat (sector/facet) or not differentiable (crease and vertex).
- **Degree-4**, when 4 creases intersect at one point (vertex).

6.2.2 Parts

- **Vertex**: the point that the 4 creases meet. Named O.
- **Crease**: a non-differentiable part that forms a ray. There are 4 sectors around a vertex, named y_i in clockwise order. y_i sometimes also refers to its intersection point with the unit sphere. It is mapped as Γ_i in the Gauss map. See Figure 2.
- **Folding angle** around a crease: how much the paper is bent around this crease. The folding angle around crease y_i is named γ_i. The folding angle *is not* the angle between sectors surfaces; its magnitude is the difference between π and the angle between adjacent sectors. See Figure 3.
- A folding angle is a **valley**, if it looks like a valley from the top; it is a **mountain** if it looks like a mountain from the top. Formally, it is a valley if the folding angle is positive, and a mountain if it is negative. It is positive when the left part of the paper is bent up if you look from the opposite direction of the ray (look from the side), and negative when the left part of the paper is bent down.
- **Sector**: a flat part of the paper, bounded by creases. There are 4 sectors around a vertex, named α_i in clockwise order. α_i sometimes also refers to its intersection arc with the unit sphere. It is mapped as A_i in the Gauss map.
- **Sector angle** for a sector: the angle between the two rays bounds this sector. It is the same as the length of α_i due to the nature of the unit sphere.
- **Gauss Map** for a curve C on a 2D surface in 3D space: For every point p on the curve C, map p to the unit vector that is normal to the surface at p and has initial point O. Then the terminal point of the vectors will form a set on the unit sphere. In performing the Gauss map to a rigid origami surface, when the magnitudes of folding angles are between 0 and π, the map will form a bowtie-ish shape, as shown in Figure 8. In the case that all folding angles are 0 or $\pm\pi$, we will have degenerate cases. See Figure 8 in the paper.

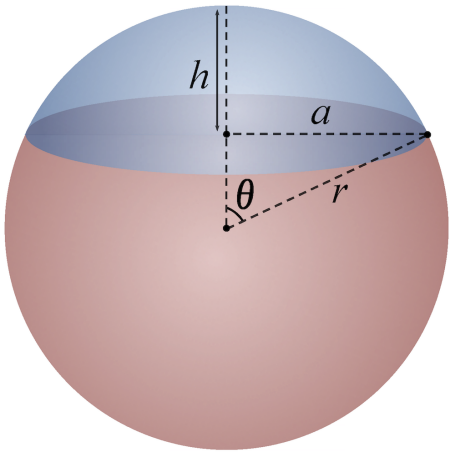

Figure 20: A spherical cap with radius and polar angle marked.

6.2.3 Other Terminologies

- **Line**: a great circle. A great circle is a circle on the sphere that has the greatest possible radius.
- **Line segment**: a segment of a great circle. it is the shortest path between two points. It is usually not called *arc* to distinguish it from a segment of a non-great circle.
- $|l|$ refers to the length of line segment l. $|AB|$ refers to the length of line segment AB.
- $|l, A|$ refers to the distance between line l and point A.

6.3 Quick Facts

This section listed some basic facts that are used in the paper without an introduction or illustration. Most of them can be found by a simple web search or in undergraduate textbooks such as [BEG99] or [Lan18].

Spherical Area

The area, or spherical excess, of a spherical triangle $\triangle ABC$ is

$$E = \angle A + \angle B + \angle C - \pi$$

Area for spherical cap) As shown in Fig20, for a spherical cap on a sphere with radius r and polar angle θ, its area is

$$E = 2\pi r^2(1 - \cos\theta)$$

Spherical Cosine Law

In a spherical triangle $\triangle ABC$ with side lengths a, b, and c, and opposite angle A, B, and C, respectively,

$$\cos a = \cos b \cos c + \sin b \sin c \cos A$$

Spherical Sine Law

In a spherical triangle $\triangle ABC$ with side lengths a, b, and c, and opposite angle A, B, and C, respectively,

$$\frac{\sin A}{\sin a} = \frac{\sin B}{\sin b} = \frac{\sin C}{\sin c}$$

Addition Formula for Sine

$$\sin(a + b) = \sin a \cos b + \sin b \cos a$$

Pythagorean identity

$$\sin^2(a) + \cos^2(a) = 1$$

Weierstrass Substitution (Tangent half-angle substitution)

$$\sin(x) = \frac{2 \tan \frac{x}{2}}{1 + \tan \frac{x}{2}}$$

, and

$$\cos x = \frac{1 - \tan \frac{x}{2}}{1 + \tan \frac{x}{2}}$$

6.4 Theorems

This section listed all major results appeared in this paper.

3.1 Sector Angles: Kawasaki's Theorem

Opposite sector angles in a flat-foldable degree-4 vertex sum up to π. That is,

$$\alpha_1 + \alpha_3 = \alpha_2 + \alpha_4 = \pi$$

.

3.2 Valley-Mountain Pattern: Maekawa's Theorem

The difference between the number of mountains and the number of valleys in a flat-foldable vertex must be 2.

3.3 Opposite Folding Angles

The opposite folding angles in a rigid folding of a degree-4 flat-foldable vertex have the same magnitude. That is,

$$\gamma_2 = -\gamma_4$$

$$\gamma_1 = \gamma_3$$

3.4 Adjacent Folding Angles

The following equation that relates adjacent folding angles and adjacent sector angles in a rigid folding of a flat-foldable, degree-4 vertex holds:

$$\frac{\tan\frac{\gamma_1}{2}}{\tan\frac{\gamma_2}{2}} = \frac{\sin\frac{\alpha_2+\alpha_1}{2}}{\sin\frac{\alpha_2-\alpha_1}{2}}.$$

3.5.1 Gauss Map for Degree-4 Vertex

For all $i = 1, 2, 3, 4$,

$$\Gamma_i = \gamma_i$$

$$\angle A_1A_2A_3 = \angle A_3A_4A_1 = \alpha_4 = \pi - \alpha_2$$

$$\angle A_2A_3A_4 = \angle A_4A_1A_2 = \alpha_1 = \pi - \alpha_3$$

3.6.2 Gauss' Remarkable Theorem

The total area of the Gauss map for a degree-4 flat-foldable vertex is 0; the areas of the two triangles that the bowtie consists of are the same in magnitude but opposite in sign.

4.1 Midpoint Collinearity Theorem

In the Gauss map image of a rigid folding of a degree-4 vertex, the midpoints of bowtie sides Γ_1, Γ_2, Γ_3, and Γ_4 are colinear.

Lemma 1

For a spherical triangle $\triangle ABC$ with all sides shorter than π and a line e intersecting it but not tangent to it, $|e, A| = |e, B| = |e, C|$, if and only if e passes through two midpoints of the side of $\triangle ABC$.

Lemma 2

Let $\triangle ABC$ be a spherical triangle. Then there exists a small (i.e., not great) circle, called Lexell's circle, such that for any point D on Lexell's circle and on the same side of the great circle made by arc BC as A, we have that the spherical area of $\triangle DBC$ equals the area of $\triangle ABC$. The Lexell's circle is defined by point A, the antipodal point of B, and the antipodal point of C.

Theorem 4.2

For spherical triangles, $\triangle ABC$ and $\triangle DBC$ with all sides shorter than π that share the same base and non-zero overlapping area, the midpoints of their distinct sides are colinear if they have the same area.

References

[BEG99] David A. Brannan, Matthew F. Esplen, and Jeremy J. Gray. *Geometry*. London, UK: Cambridge University Press, 1999.

[FHR22] Johnna Farnham, Thomas C. Hull, and Aubrey Rumbolt. "Rigid folding equations of degree-6 origami vertices". In: *Proceedings of the Royal Society, Series A* 478.2260 (2022), p. 20220051. DOI: 10.1098/rspa.2022.0051.

[Gha] Amanda Ghassaei. *Origami Simulator*. https://origamisimulator.org. Accessed: 4-30-2024.

[Hoh] Markus Hohenwarter. *GeoGebra*. https://www.geogebra.org. Accessed: 4-30-2024.

[Huf76] David A. Huffman. "Curvature and creases: a primer on paper". In: *IEEE Transactions on Computers* C-25.10 (1976), pp. 1010–1019.

[Hul20] Thomas C. Hull. *Origametry: Mathematical Methods in Paper Folding*. New York, NY: Cambridge University Press, 2020.

[Hul94] Thomas C. Hull. "On the mathematics of flat origamis". In: *Congressus Numerantium* 100 (1994), pp. 215–224.

[KT88] Kunihiko Kasahara and Toshi Takahama. *Origami for the Connoisseur*. Tokyo: Japan Publications, 1988.

[Lan18] Robert J. Lang. *Twists, Tilings, and Tessellations: Mathematical Methods for Geometric Origami*. Boca Raton, FL: A K Peters/CRC Press, 2018.

[LMH16] Robert J. Lang, Spencer Magleby, and Larry Howell. "Single Degree-of-Freedom Rigidly Foldable Cut Origami Flashers". In: *Journal of Mechanisms and Robotics* 8.3 (Mar. 2016). 031005, 031005 (15 pages). ISSN: 1942-4302. DOI: 10.1115/1.4032102. URL: https://doi.org/10.1115/1.4032102.

[ONe66] Barrett O'Neill. *Elementary Differential Geometry*. New York, NY: Academic Press, 1966.

[Rob78] S. A. Robertson. "Isometric folding of Riemannian manifolds". In: *Proceedings of the Royal Society of Edinburgh* 79.3–4 (1977–1978), pp. 275–284.

[Tod14] Isaac Todhunter. *Spherical Trigonometry for the Use of Colleges and Schools*. London, UK: London Macmillan, 1914.